The lysosomal signaling anchor p18/LAMTOR1 controls epidermal development by regulating lysosome-mediated catabolic processes

Taeko Soma-Nagae*, Shigeyuki Nada*, Mari Kitagawa, Yusuke Takahashi, Shunsuke Mori, Chitose Oneyama and Masato Okada‡

Department of Oncogene Research, Research Institute for Microbial Diseases, Osaka University, 3-1 Yamadaoka, Suita, Osaka 565-0871, Japan

*These authors contributed equally to this work
‡Author for correspondence (okadam@biken.osaka-u.ac.jp)

Accepted 28 May 2013
Journal of Cell Science 126, 3575–3584

doi: 10.1242/jcs.121913

Summary

The lysosomal adaptor protein p18 is an essential anchor of a scaffolding complex for the mTORC1 and MAPK pathways, which play crucial roles in controlling cell growth and energy homeostasis. To elucidate the *in vivo* function of the p18-mediated pathway, we conditionally ablated p18 in the mouse epidermis. Mutant mice were born with severe defects in formation of the stratum corneum and died within 12 h after birth due to dehydration caused by loss of skin barrier function. Mutant epidermal cells can grow and differentiate into granular cells, but exhibit functional defects in corneocyte maturation. Electron microscopy identified abnormal immature cells, overlying the mutant granular cells, which accumulated autophagosomes, glycogen granules and dead nuclei. Cell culture analysis showed that loss of p18 attenuated lysosome function, resulting in accumulation of immature lysosomes and autophagosomes. Analyses of lysosome behavior revealed that p18 is required for functional interaction between lysosomes and target organelles including autophagosomes. These findings suggest that p18-mediated pathways control lysosome-mediated catabolic processes, which are crucial for the development of mouse epidermis.

Key words: p18, mTORC1, Lysosomes, Autophagy, Epidermis

Introduction

To survive and respond to environmental cues, cells import nutrients and extracellular macromolecules via the endosome system. Endocytosed materials are first delivered to early endosomes, where they are sorted; subsequently they are either recycled to the cell surface or targeted for degradation (Huotari and Helenius, 2011; Luzio et al., 2007). Materials fated for degradation are transported to late endosomes (Falguières et al., 2008; Falguières et al., 2009), which subsequently fuse with primary lysosomes, forming late endosome–lysosome hybrids, i.e. mature lysosomes (Luzio et al., 2007). These mature lysosomes accumulate in the perinuclear compartment by associating with microtubules (Harada et al., 1998), and digested materials are either released into the cytoplasm or exocytosed. Under starved conditions, cells degrade intracellular components by autophagy to regenerate metabolic precursors that are recycled for macromolecular synthesis and ATP generation (Mizushima et al., 2011). Autophagosomes that have engulfed cellular components fuse with lysosomes to form autolysosomes, in which components are degraded by lysosomal hydrolases. Many secreting cells contain cell type-specific lysosome-related organelles (LROs), such as melanosomes and lamellar bodies, which contain lysosomal enzymes required for macromolecule processing and secretion (Bonifacino, 2004; Dell'Angelica et al., 2000). Together, these lysosome-related endosome systems are crucial for the maintenance of cell homeostasis, as well as cell type-specific functions such as the processing of secretory macromolecules. However, the regulatory mechanisms underlying lysosome-mediated cellular functions remain elusive.

The endosome system is associated with intracellular signaling (Miaczynska et al., 2004). Components of a branch of the MAPK pathway are recruited to late endosomes via the p14–MP1 complex, which serves as a MEK1-specific scaffold (Teis et al., 2002). Ablation of the p14–MP1 complex results in aberrant subcellular distribution and trafficking of late endosomes (Bohn et al., 2007; Teis et al., 2006), suggesting that the p14–MP1-mediated pathway is involved in the regulation of endosome/lysosome biogenesis. Recently, we identified a novel membrane adaptor protein, p18 (also LAMTOR1), which specifically binds to the p14–MP1 complex (Nada et al., 2009). p18 is exclusively localized to late endosomes/lysosomes and acts as an essential anchor for the p14–MP1 complex. The p18–p14–MP1 complex is highly conserved from yeast to humans (Kogan et al., 2010), indicating that it plays a critical role in eukaryotic cells. p18-deficient mouse embryos die during early developmental stages with severe defects in endosome/lysosome organization and membrane–protein transport in the visceral endoderm (Nada et al., 2009). Analysis of p18-deficient cells suggests that the p18–p14–MP1 complex plays a crucial role in controlling cell growth and endosome dynamics, including membrane–protein transport and lysosome biogenesis.

More recently, the p18–p14–MP1 complex was found to serve as a scaffold (Ragulator) for the Rag GTPase complex (RagAB/CD), which is required for amino acid-dependent activation of

Journal of Cell Science

the mammalian target of rapamycin complex 1 (mTORC1) on lysosomes (Sancak et al., 2010; Zoncu et al., 2011a). To respond to amino acid levels, the Ragulator functionally interacts with lysosomal v-ATPase (Zoncu et al., 2011b) and forms a complex with HBXIP and C7orf59 to serve as a GEF for Rag GTPases (Bar-Peled et al., 2012). These findings demonstrate that the p18–p14–MP1–Rag complex is essential for controlling the activity of mTORC1, and indicate that the complex plays a crucial role in controlling cell growth by promoting protein translation. On the other hand, we recently showed that p18-mTORC1 activity is also involved in the regulation of lysosomal function by controlling lysosomal maturation (Takahashi et al., 2012). Furthermore, other groups have proposed potential roles of p18 in cellular cholesterol homeostasis (Guillaumot et al., 2010) and p53-dependent apoptosis via aberrant lysosomal activation (Malek et al., 2012). These *in vitro* observations suggest the importance of the p18-related complex in the regulation of the lysosome system, but its *in vivo* function and the sites of its action remain unknown.

To elucidate the function of the p18-related complex, we conditionally ablated p18 in moue epidermis. Mutant epidermis exhibited severe defects in formation of the stratum corneum, accompanied by functional defects in granular cells. Analyses of tissues and keratinocytes revealed that the p18-related complex is required for promoting lysosome-mediated degradation of cellular components, including autophagosomes and endocytosed materials. Our observations of lysosome dynamics further showed that the p18 complex is involved in regulating functional interaction between lysosomes and target organelles, e.g. autolysosome formation. These findings suggest that the p18-related complex controls lysosome-mediated catabolic processes, which is crucial for development of mouse epidermis.

Results

Ablation of p18 in the epidermis

p18 is expressed ubiquitously (Nada et al., 2009), but it is highly concentrated in epithelial and exocrine tissues, such as the gastrointestinal tract, epidermis and pancreas (data not shown). Therefore, to address the *in vivo* function of p18, we conditionally ablated p18 in epidermal basal cells. $p18^{flox/flox}$ mice, in which exon 1 of the p18 gene is flanked by loxP sites (Fig. 1A), were crossed with *Keratin 5-Cre* (*K5-Cre*) transgenic mice (Tarutani et al., 1997), and F2 offspring or embryos (E17.5) were genotyped by PCR (Fig. 1B). The elimination of p18 protein in the mutant epidermis was confirmed by immunohistochemistry (Fig. 1C). *Keratin 5-Cre* $p18^{flox/flox}$ [$k5p18^{-/-}$; knockout (KO)] mice were born at the expected Mendelian ratio, but neonates died within 12 h after birth with dramatic skin defects. The skin of mutant mice was generally very thin and adhesive, and their eyelids were absent. Mutant embryos at E17.5 exhibited additional defects; the skin of heterozygous control $k5p18^{+/-}$ embryos dried soon after caesarean section, whereas the skin of KO $k5p18^{-/-}$ embryos was continuously humid. Mutant KO neonates rapidly died within a couple of hours, before skin dried (Fig. 1D). These results suggest that loss of p18 affects skin barrier function, which protects against leakage of body fluid. Indeed, an epidermal barrier assay based on the permeability of X-gal revealed that the skin of mutants completely lacked barrier function (Fig. 1E). Hematoxylin-eosin (HE) staining of skin sections revealed that the control epidermis exhibited a prototype

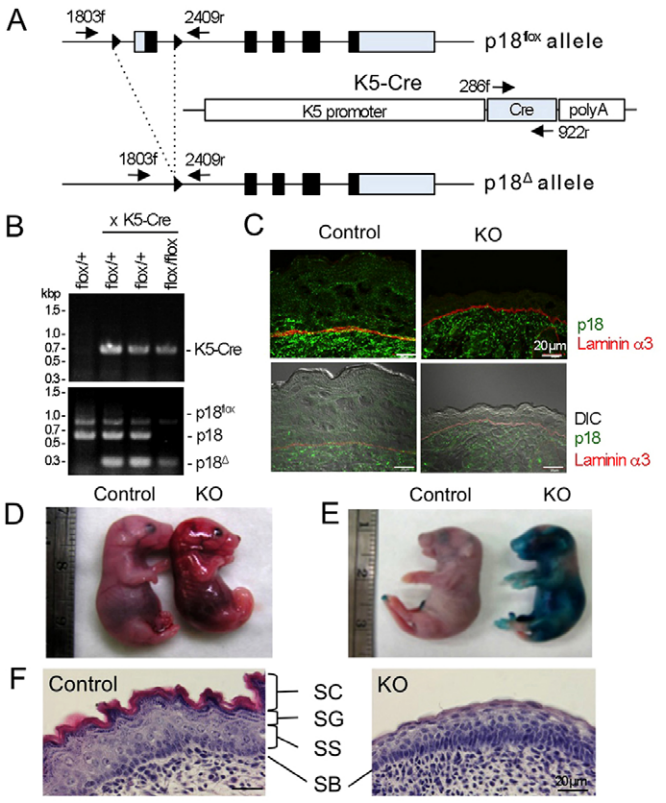

Fig. 1. Ablation of p18 in the epidermis. (**A**) The floxed and deleted *p18* alleles and the K5-Cre transgene construct are shown. Arrows indicate primers for genotyping. (**B**) PCR genotyping of tail DNA from E18.5 $p18^{flox/+}$, K5-Cre $p18^{flox/+}$ and K5-Cre $p18^{flox/flox}$ embryos. (**C**) Immunofluorescence staining of control and p18 KO epidermis using antibodies against p18 and laminin α3. (**D**) External appearances of the indicated genotypes of E17.5 embryos removed by caesarean section. (**E**) Epidermal barrier assay with X-gal on newborn mice of the indicated genotypes. (**F**) Hematoxylin-eosin (HE) staining of epidermal sections from E17.5 embryos of the indicated genotypes. SC, stratum corneum; SG, stratum granulosum; SS, stratum spinosum; SB, stratum basale.

stratified squamous epithelium that was stably covered by the stratum corneum (SC), whereas the mutant epidermis was very thin and consisted of only a few (2–4) cell layers (Fig. 1F). Notably, the mutant epidermis completely lacked the stratum corneum.

Defects in epidermal organization upon loss of p18

To elucidate the molecular basis for the epidermal defects resulting from loss of p18, we examined differentiation of the epidermis by immunofluorescence (Fig. 2A). Staining for laminin α3 indicated that formation of the basement membrane is not affected by loss of p18. Keratin 5 was positive in the undifferentiated basal layers of the epidermis in mice of both genotypes. In addition, staining for the cell-proliferation marker Ki67 was almost identical in the basal cell layers of both genotypes. These results indicate that basal cells develop normally even in the absence of p18.

Keratin 1, a component of keratin fibers in the spinous and granular layers of the epidermis, was also detected in the mutant epidermis, although the thickness of the keratin 1-positive cell layers, particularly the granular layers, was greatly reduced in the

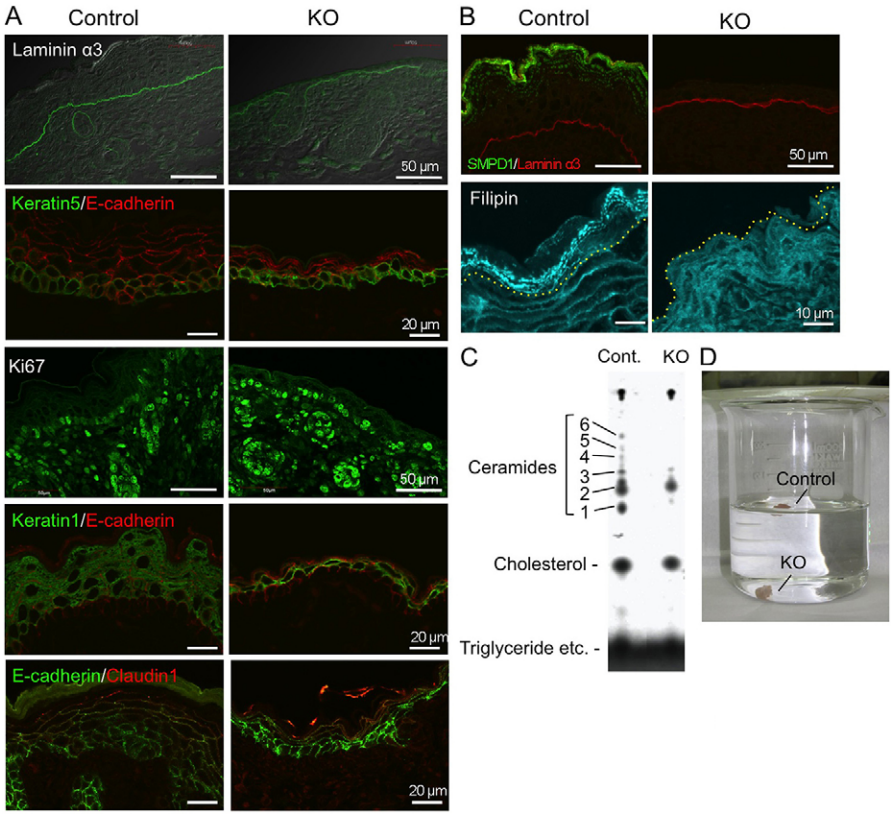

Fig. 2. Defects in epidermal organization upon loss of p18. (**A**) Immunofluorescence staining of wild-type (control) or mutant (KO) epidermis for the indicated marker proteins. (**B**) Fluorescent staining of wild-type (control) or mutant (KO) epidermis with anti-SMPD1 and anti-laminin α3 antibodies (upper) and filipin (lower). The interface between granular cells and the stratum corneum is indicated by yellow dotted lines. (**C**) Thin-layer chromatogram of lipids extracted from wild-type (control) or mutant (KO) epidermis. (**D**) Epidermal tissues from wild-type (control) or mutant (KO) mice were soaked in phosphate-buffered saline in a beaker.

mutant, suggesting that loss of p18 causes some defect in the granular layers. In both wild-type and mutant epidermis, E-cadherin and claudin-1 were detected at cell–cell junctions in the spinous and granular layers. Thus, formation of cell–cell junctions, such as adherens junctions and tight junctions, may not be dramatically affected by loss of p18. These observations indicate that the mutant epidermal cells can grow and differentiate into granular cells. However, loss of p18 impairs some function of granular cells, and this impairment may be linked to defective formation of the stratum corneum in the mutant epidermis.

Defects in the stratum corneum upon loss of p18

Based on these findings, we focused our analysis on the effects of loss of p18 on the processes of stratum corneum formation by granular cells. The stratum corneum is the outermost layer of the epidermis, consisting of terminally differentiated corneocytes that lack nuclei and organelles (supplementary material Fig. S1). Corneocytes are hexagonal cells packed mainly with keratin filaments bundled with filaggrin, and are surrounded by a cornified cell envelope composed of involucrin and loricrin, which are cross-linked by transglutaminase 1 (TGM1) and covalently bound to lipids. The inter-corneocyte space is filled mostly with ceramides and cholesterol, as well as several catabolic enzymes that are secreted from granular cells via lamellar bodies (Bouwstra et al., 2003).

To investigate the effects of loss of p18 on the formation of stratum corneum, we determined the contents of the inter-corneocyte space, i.e. hydrolytic enzymes and lipids, which are secreted via lamellar bodies (supplementary material Fig. S1). One such component, sphingomyelin phosphodiesterase 1 (SMPD1) catalyzes hydrolysis of sphingomyelin to produce ceramides. Immunofluorescence revealed that in control epidermis, most of the SMPD1 was detected in the inter-corneocyte space, whereas it was not detectable in mutant epidermis (Fig. 2B, upper). Cholesterol was also detected in the stratum corneum only in control epidermis (Fig. 2B, lower). Furthermore, analysis of lipids in the epidermis showed that the levels of cholesterol and ceramides were dramatically reduced in the mutant epidermis (Fig. 2C). Due to the loss of lipids, mutant skin sank in phosphate buffer solution, whereas control skin floated on the surface (Fig. 2D). These observations suggest that the function and development of granular cells, i.e. production of the inter-corneocyte components, is impaired upon loss of p18.

Defects in corneocyte formation upon loss of p18

To further determine the effects of loss of p18 on the formation of corneocytes, we examined filaggrin proteins. In control epidermis, filaggrin was detected in large keratohyalin granules and adjacent to keratin patterns in the stratum corneum (Fig. 3A). In mutant epidermis, however, filaggrin signals were detected in smaller granules in a single cell layer, and no fibrous staining was detected. Furthermore, electron microscopy revealed that control epidermis contained multiple layers of granular cells that contain large keratohyalin granules, whereas the mutant epidermis consisted of a single layer of granular cells that contain smaller keratohyalin granules (Fig. 3B). These observations suggest that loss of p18 decreases the supply of filaggrin, resulting in defective formation of keratin fibers in the stratum corneum.

Over the course of these observations, we noticed that mutant epidermis contained abnormal corneocyte-like cells (termed

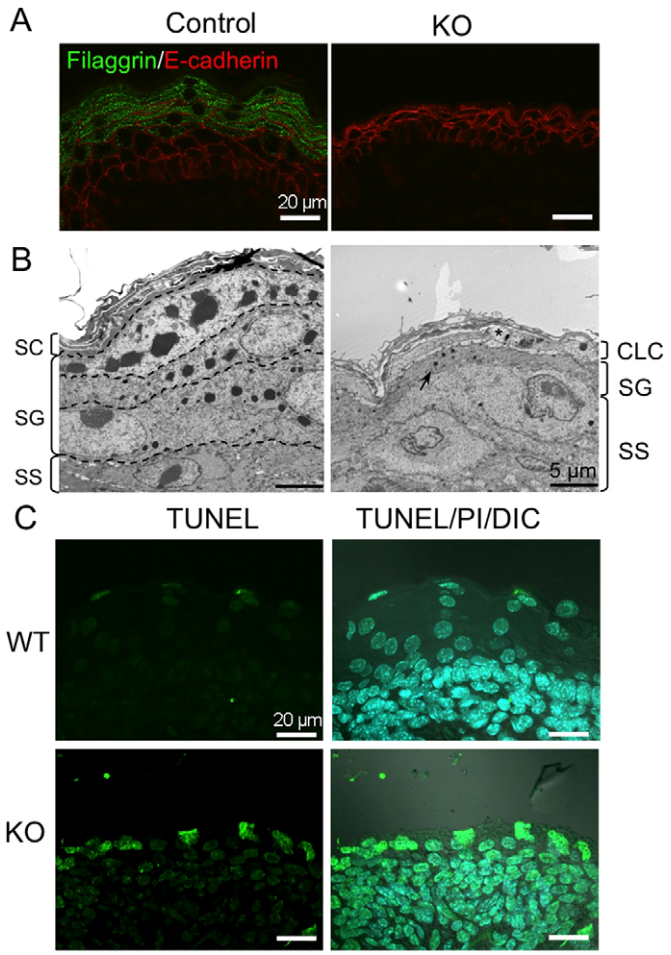

Fig. 3. Defects in corneocyte formation upon loss of p18. (**A**) Immunofluorescence staining for filaggrin of wild-type (control) or mutant (KO) epidermis. Nuclei were co-stained with propidium iodide (PI). (**B**) Electron microscopy of wild-type (control) or mutant (KO) epidermis. CLC, immature corneocyte-like cells; SC, stratum corneum; SG, stratum granulosum; SS, stratum spinosum. (**C**) Epidermal tissues from wild-type (WT) and mutant (KO) mice were subjected to TUNEL assay. Images of TUNEL-positive signals and merged images with PI staining and differential interference contrast (DIC) images are shown.

CLCs) at the upper layer of the granular cell layer (SG) in place of the stratum corneum (SC). Normally differentiated corneocytes are enucleated, but these CLCs retained their nuclei (*), as confirmed by propidium iodide (PI) staining (Fig. 3C). However, TUNEL revealed that the nuclei in these cells are TUNEL-positive, indicating that the cells are undergoing fragmentation of genomic DNA and that the nuclei are already dead (Fig. 3C). These observations suggest that loss of p18 may affect the process of disruption or autolysis of nuclei during the terminal differentiation of corneocytes.

Defects in autophagy upon loss of p18

We next characterized the abnormal CLCs in greater detail by higher-resolution electron microscopy. We found that these abnormal cells accumulated autophagosome-like structures (Fig. 4A). Immunofluorescence staining for LC3 puncta, a marker of autophagosomes, also revealed that LC3-positive autophagosomes were accumulated in the outermost layers of the mutant epidermis (Fig. 4B). Furthermore, we identified accumulations of unstructured materials, organelles and glycogen granules in the mutant cells (Fig. 4C). These unusual accumulations of undigested materials suggest that loss of p18 suppresses degradation of cellular components via autophagy and/or the endosome system.

To address this possibility, we examined the effects of loss of p18 on autophagy in primary keratinocytes (Fig. 4D). Wild-type and mutant keratinocytes prepared under nutrient-rich conditions were amino acid-starved for 1 h and then the media were replaced with a nutrient-rich medium to allow the cells to recover for up to 40 min. Even under nutrient-rich conditions, the number of LC-3 positive puncta was significantly increased in cells lacking p18. Under starved conditions, autophagosome formation was greatly induced in both cell types, indicating that the initiation of autophagosome formation is not affected by loss of p18. When cells were returned to nutrient-rich media, autophagosomes rapidly disappeared in wild-type keratinocytes, whereas greater numbers of autophagosomes were retained in mutant keratinocytes (Fig. 4E). Electron microscopy of keratinocytes confirmed the accumulation of autophagosomes in mutant keratinocytes (Fig. 4F). Based on these observations, we hypothesize that loss of p18 suppresses the process of autophagosome degradation that is mediated by lysosomes.

Defects in lysosomal function upon loss of p18

To further investigate the above possibility, we used p18-deficient mouse embryonic fibroblasts (MEFs) established from $p18^{flox/flox}$ mouse embryos. Autophagy was induced by depleting nutrients, and autophagosomes were detected by staining for LC-3 and p62, another marker of autophagosome formation, on the same schedule as used for keratinocytes (Fig. 5A). Mutant fibroblasts also exhibited a significant increase in the number of basal autophagosomes, and retained greater numbers of autophagosomes, even when the cells were returned to nutrient-rich media (Fig. 5B,C). Western blot analysis for LC3-I/II also revealed that degradation of autophagosomes was suppressed by loss of p18 (Fig. 5D). When cells were starved for up to 24 h, degradation of autophagosomes and LC3 were suppressed in cells lacking p18 (supplementary material Fig. S2). These findings demonstrate that loss of p18 causes defects in autophagosome degradation.

In a previous study, we showed that loss of p18 affects the distribution and maturation of lysosomes (Takahashi et al., 2012). In the p18-deficient MEFs used in this study, Lamp1-positive lysosomes were widely distributed in the cytoplasm, whereas in wild-type MEFs only a limited number of Lamp1-positive lysosomes accumulated in the perinuclear compartment (Fig. 6A). Western blot analysis revealed that Lamp1 and mature cathepsin D1, but not other endosomal markers such as Rab5 and Rab11 (Takahashi et al., 2012), dramatically accumulate in p18 KO cells (Fig. 6B). The accumulation of mature cathepsin D1 in p18 KO cells also indicated that acidification of lysosomes was not affected by loss of p18. Indeed, analyses with pH indicators revealed that there was no significant difference in lysosomal pH between wild-type and mutant cells (data not shown). These results suggest that in the absence of p18, immature lysosomes specifically accumulate due to the defects in lysosome maturation processes.

To explore this possibility, we treated cells with bafilomycin A1 (BafA1), which attenuates lysosome function by inhibiting

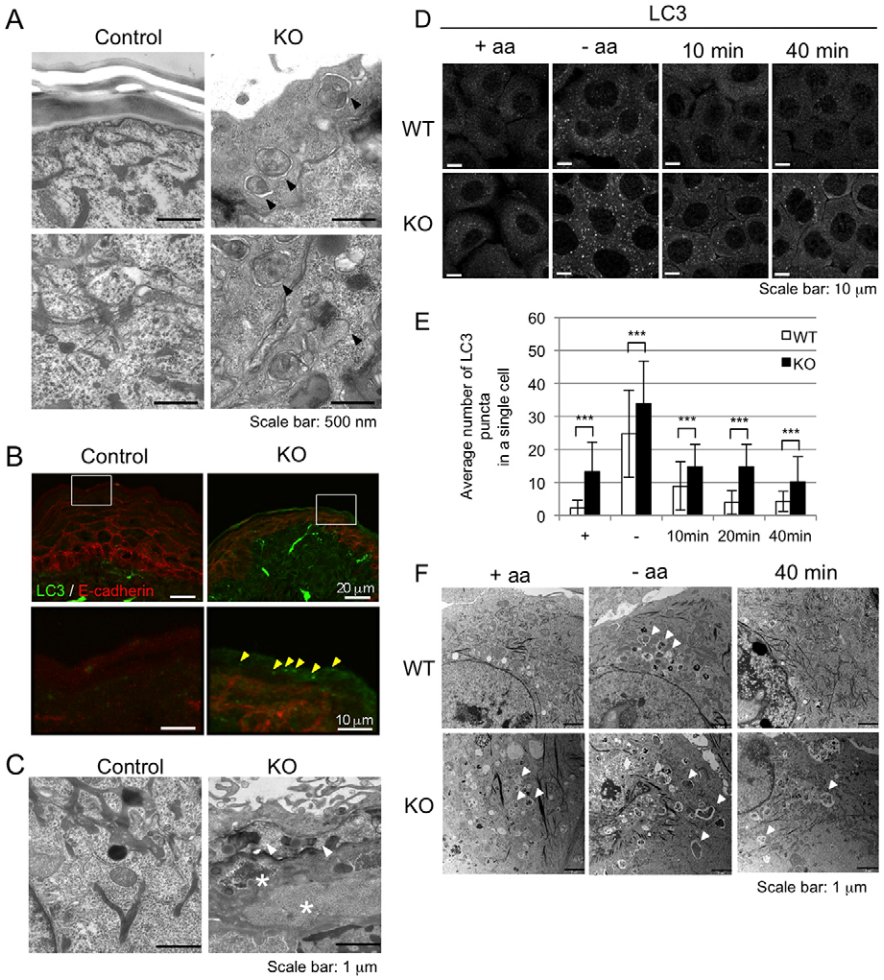

Fig. 4. Loss of p18 causes autophagosomes to accumulate in the epidermis. (**A**) Upper: electron microscopy of corneocytes in wild-type (control) and immature corneocyte-like cells in mutant (KO) epidermis. Lower: electron microscopy of granular cells in wild-type (control) and mutant (KO) epidermis. Arrowheads indicate autophagosome-like structures. (**B**) Upper: LC3 staining of the surface areas of the epidermis in wild-type (control) or mutant (KO) epidermis. Lower: magnified views of boxed areas in the upper images. Yellow arrowheads indicate LC3-positive autophagosomes. (**C**) Electron microscopy of granular cells in wild-type (control) and immature corneocyte-like cells in mutant (KO) epidermis. White arrowheads indicate unstructured organelles. White asterisks indicate glycogen granules. (**D**) Wild-type (WT) and mutant (KO) keratinocytes prepared under nutrient-rich conditions were starved for 1 h under amino acid-starved conditions and then the media were replaced with nutrient-rich media to allow the cells to recover. At the indicated time points, autophagosomes were detected by immunofluorescence staining for LC3. + aa, nutrient-rich conditions; − aa, amino acid-starved conditions. (**E**) The numbers of LC3 puncta were counted for 50 cells and average numbers ± s.d. in a single cell at the indicated times are shown. ***$P<0.001$ by Student's *t*-test. (**F**) Keratinocytes cultured as in D were observed by electron microscopy. White arrowheads indicate autophagosomes.

vacuolar H^+ ATPase (V-ATPase) (Yamamoto et al., 1998). In both wild-type and mutant cells, treatment with BafA1 did not affect the expression of Lamp1 or mature cathepsin D1 (Fig. 6B), indicating that lysosome assembly is not affected by BafA1 treatment. Prior to BafA1 treatment, wild-type cells contained only low levels of LC3-II (Fig. 6B) and autophagosomes (Fig. 6C,D), but BafA1 treatment induced dramatic (~20-fold) accumulation of autophagosomes. This result indicates that in wild-type cells, autophagy is actively induced and autophagosomes are rapidly degraded through lysosomes. On the other hand, mutant cells contained substantial numbers of autophagosomes even before BafA1 treatment; consequently, the drug facilitated accumulation of autophagosomes (Fig. 6B–D). This additive effect (~3-fold) suggests that lysosome-mediated autophagosome degradation does take place in the mutant cells. However, based on the fact that mutant cells substantially accumulated autophagosomes without BafA1 treatment, even despite the excessive accumulation of immature lysosomes, it is likely that the efficiency of lysosome-mediated degradation of autophagosomes is greatly reduced upon loss of p18. We further verified the defect in lysosome function resulting from loss of p18 by performing a DQ-Red BSA analysis, which revealed that the efficiency of lysosomal degradation of endocytosed materials is also attenuated in mutant cells (supplementary material Fig. S3). Taken together, these findings suggest that loss of p18 inactivates function of lysosomes that target autophagosomes as well as late endosomes.

Defects in functional interaction between lysosomes and autophagosomes upon loss of p18

To address the mechanism of action of the p18 complex, we observed behaviors of organelles positive for p18, Lamp1 and LC3. Time-lapse analyses of cells expressing p18-GFP and Lamp1-mCherry showed that p18 exclusively co-localizes with Lamp1 on lysosomes (supplementary material Fig. S4; Movie 1), indicating that the p18-associated complex acts on lysosomes to regulate their functions. Co-expression analyses of Lamp1-mCherry and LC3-GFP revealed that in wild-type cells, Lamp1-positive lysosomes dynamically extended and retracted tubular branches and moved rapidly along microtubules (Fig. 7A; supplementary material Movies 2–5). We also observed that Lamp1-positive lysosomes occasionally and temporally interact with LC3-positive autophagosomes, potentially via kiss-and-run interactions (Fig. 7A, insets) that are critical for autolysis (Jahreiss et al., 2008). In contrast, in mutant cells, Lamp1-positive lysosomes were distributed widely throughout the cytoplasm, rarely formed tubular structures and moved slowly, particularly in the peripheral area of the cells (Fig. 7A). The efficiency of inter-vesicular interaction was further analyzed by scoring the incidence and duration of Lamp1-mCherry and LC3-GFP colocalization. For these analyses, LC3-GFP was transiently expressed in p18 KO cells (KO) and p18 re-expressing cells (Rev) that stably express Lamp1-mCherry. The incidences of longer kiss-and-run interactions tended to be reduced in KO cells

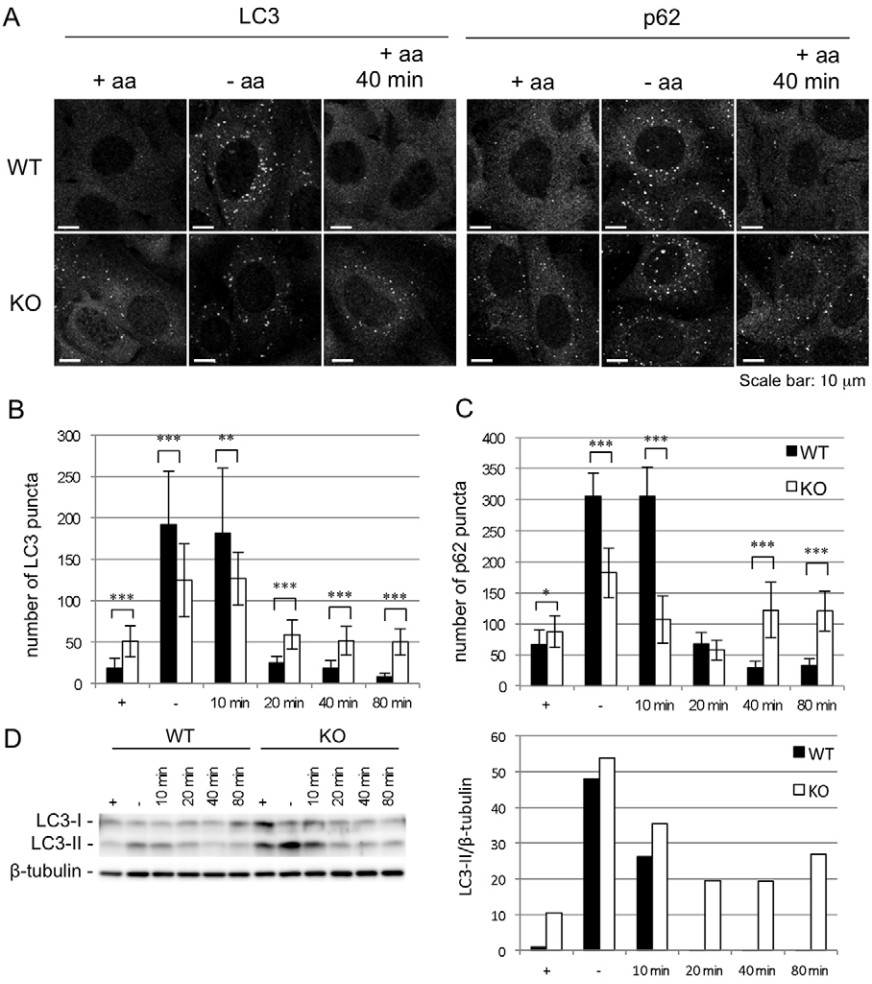

Fig. 5. Loss of p18 suppresses degradation of autophagosomes in fibroblasts. (**A**) Wild-type (WT) and mutant (KO) MEFs were starved for 1 h and media were replaced with nutrient-rich media to allow the cells to recover. At the indicated time points, autophagosomes were detected by immunofluorescence staining for LC3 and p62. + aa, nutrient rich conditions; − aa, amino acid-starved conditions. (**B**) Numbers of LC3 puncta were counted for 50 cells and average numbers ± s.d. in a single cell at the indicated times are shown. ***$P<0.001$, **$P<0.01$ by Student's *t*-test. (**C**) Numbers of p62 puncta were counted for 50 cells and average numbers ± s.d. in a single cell at the indicated times are shown. ***$P<0.001$, *$P<0.05$ by Student's *t*-test. (**D**) Total cell lysates from the MEFs used in A were subjected to western blot analysis for LC3 (left panel). Band intensities of LC3-II were quantified and normalized against the levels of β-tubulin (right panel).

compared with Rev cells (Fig. 7B). It was also shown that inhibition of mTORC1 and the MAPK pathways by rapamycin and PD0325901, respectively, was able to mimic the effects of loss of p18. These findings raise the possibility that the p18 complex mediates the functional interaction between lysosomes and their target autophagosomes.

Defects in autolysosome formation upon loss of the p18 complex

To further define the action of the p18 complex, we used BafA1 to temporally accumulate autophagosomes by inhibiting autolysis. p18 KO and Rev cells were incubated with BafA1, and localizations of LC3 and Lamp1 signals were analyzed using Z-stack confocal microscopy (Fig. 8A). In Rev cells, treatment with BafA1 for 4 h induced accumulation of larger sized vacuolar-like vesicles in which LC3 and Lamp1 are mostly co-localized in the lumen of these vesicles. Longer treatment (16 h) further enlarged the double-positive vacuoles. Four hours after BafA1 was washed out to re-activate lysosome function, LC3 autophagosomes were mostly abolished, though Lamp1 vacuoles remained enlarged. These observations suggest that in the presence of p18, functional interaction, i.e. formation of autolysosomes via membrane fusion between lysosomes and autophagosomes or engulfment of autophagosomes by lysosomal vacuoles, can be accomplished even in the presence of BafA1, and autolysis is restarted by the disinhibition of lysosomal hydrolases.

In p18 KO cells, BafA1 treatment induced accumulation of larger Lamp1-positive vacuoles and increased in the number of LC3-positive autophagosomes. However, the enlargement of autophagosomes was more moderate, and some were not co-localized with vacuoles or remained attached to the surface of vacuoles. Even when BafA1 was washed out, most autophagosomes remain undigested. Essentially the same effects were reproducibly observed in other cultures (supplementary material Fig. S5). These findings suggest that loss of p18 interferes with interactions between autophagsomes and lysosomes, such as organelle fusion, consequently suppressing degradation of autophagosomes.

Finally, to assess the contribution of the p18-associated signaling pathways to lysosomal functions, we examined the effects of inhibition of mTORC1 and MAPK pathways on the functional interaction between autophagsomes and lysosomes in BafA1-treated Rev cells (Fig. 8B). In a manner quite similar to the effects observed in p18 KO cells, treatment with rapamycin attenuated formation of Lamp1-positive larger vacuoles and their co-localization with LC3-positive autophagosomes, resulting in impaired degradation of autophagosomes after BafA1 was washed out. This suggests that mTORC1 activity is crucial for executing p18-mediated functions. Furthermore, treatment with PD0325901 induced similar effects, suggesting that the activity of the MAPK pathway is also required for these cellular events. Essentially the same results were reproducibly observed in other sets of cultures (supplementary material Fig. S6).

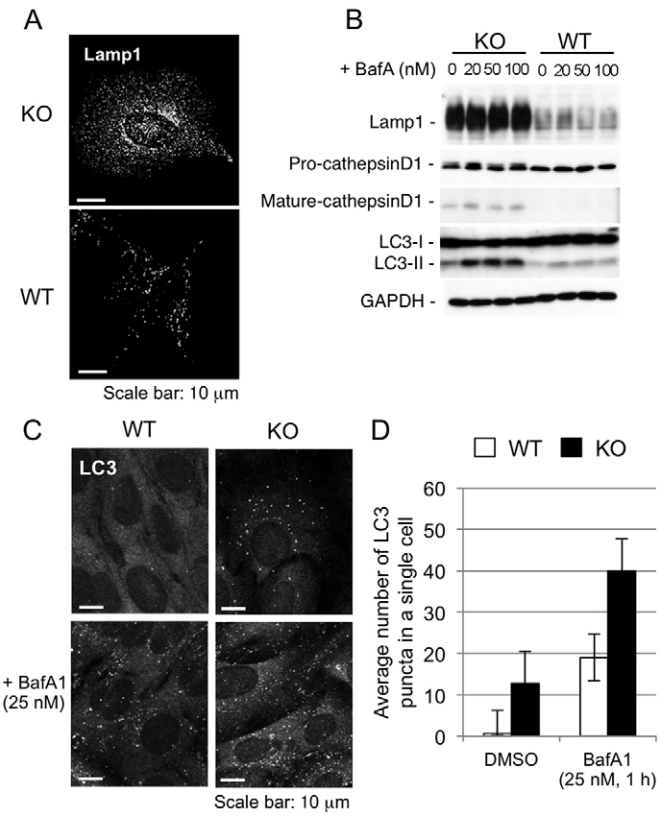

Fig. 6. Defects in lysosomal function upon loss of p18. (**A**) Immunofluorescence staining for Lamp1 in wild-type (WT) and mutant (KO) MEFs. (**B**) Wild-type (WT) and mutant (KO) MEFs were treated with the indicated concentrations of bafilomycin A1 (BafA1) for 1 h, and total cell lysates were subjected to western blot analysis for the indicated proteins. (**C**) Wild-type (WT) and mutant (KO) MEFs were treated with or without BafA1 for 1 h and stained for LC3. (**D**) Numbers of LC3 puncta in the indicated cell types were counted for 50 cells and average numbers ± s.d. in a single cell are shown.

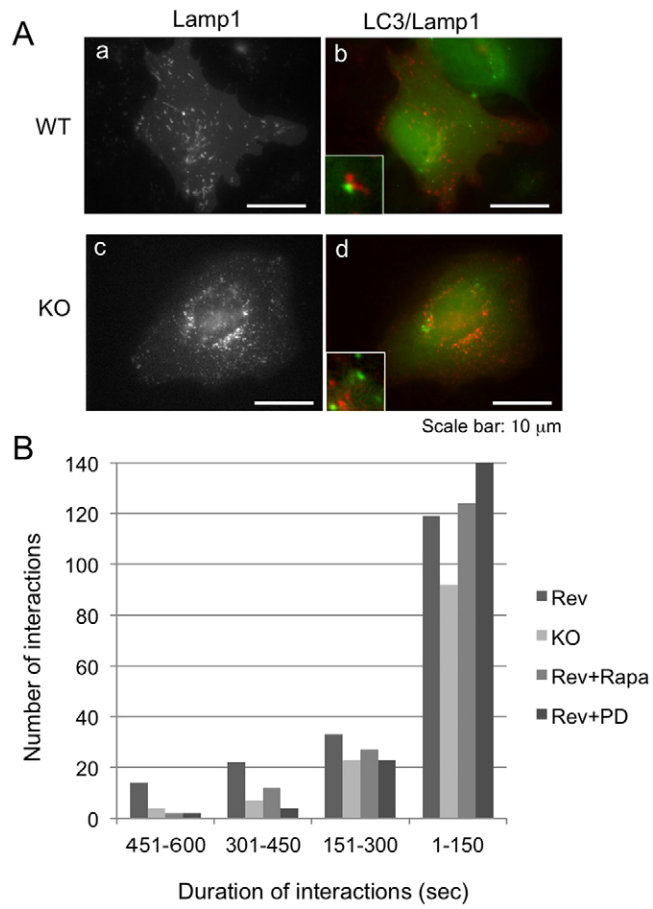

Fig. 7. Defects in interaction between lysosomes and autophagosomes upon loss of p18. (**A**) Lamp1-mCherry and LC3-GFP constructs were transiently co-transfected into wild-type (WT) and mutant (KO) MEFs and their behaviors were observed by time-lapse microscopy (supplementary material Movies 2–5). Initial images of Lamp1-mCherry (white) and LC3/Lamp1 (green/red) are shown. Insets show magnified views of interaction between Lamp1- and LC3-positive vesicles. (**B**) From the time-lapse images, frequency of the kiss-and-run interactions was scored by manually counting the number of colocalizations of Lamp1-mCherry and LC3-GFP signals and the duration of each interaction in six independent cells. Total numbers of interactions were plotted as a function of duration (sec).

Taken together, these findings suggested that the p18-associated pathways, mTORC1 and/or MAPK pathways, are involved in promoting functional interactions between lysosomes and target organelles to regulate lysosome-mediated catabolic processes (Fig. 8C) which are crucial for maintenance of cell homeostasis and cell fate determination such as formation of the stratum corneum during epidermal development.

Discussion

To address the *in vivo* function of the p18 complexes, we examined the effects of loss of p18 on epidermal development. The mutant epidermis exhibited severe defects, particularly in development of the stratum corneum, causing a loss of skin barrier function. Histology revealed that loss of p18 abrogated the formation of corneocytes; in their place appeared immature corneocyte-like cells that contained various undigested components such as dead nuclei, autophagosomes and glycogen granules. In previous work, we showed that wild-type visceral endoderm (VE) cells in normal embryos develop huge lysosome-like vacuoles (‘giant lysosomes’), whereas p18-deficient VE cells fail to form these structures and instead accumulate smaller lysosome-like organelles filled with amorphic materials (Nada et al., 2009). These findings suggest that the p18 complex plays general and critical roles in controlling lysosome-mediated catabolic processes.

We showed that the p18 complex is required for functional interaction between lysosomes and their targets, such as autophagosomes and late endosomes, to promote lysosomal degradation processes. Analyses of BafA1-treated cells revealed that loss of p18 complexes attenuates autolysosome formation potentially by suppressing lysosomal fusion. This raises the possibility that the p18 complex regulates functions of molecules involved in controlling specific vesicular interaction with lysosomes (Bonifacino and Rojas, 2006; Johannes and Wunder, 2011; Wickner and Schekman, 2008; Yu et al., 2010). Lysosomal fusion requires various components, including SNARE proteins, Rab GTPases and SNARE-associated proteins (SM proteins, NSF, SNAP and others) (Luzio et al., 2007). The functions of some components are regulated by phosphorylation (Wickner and

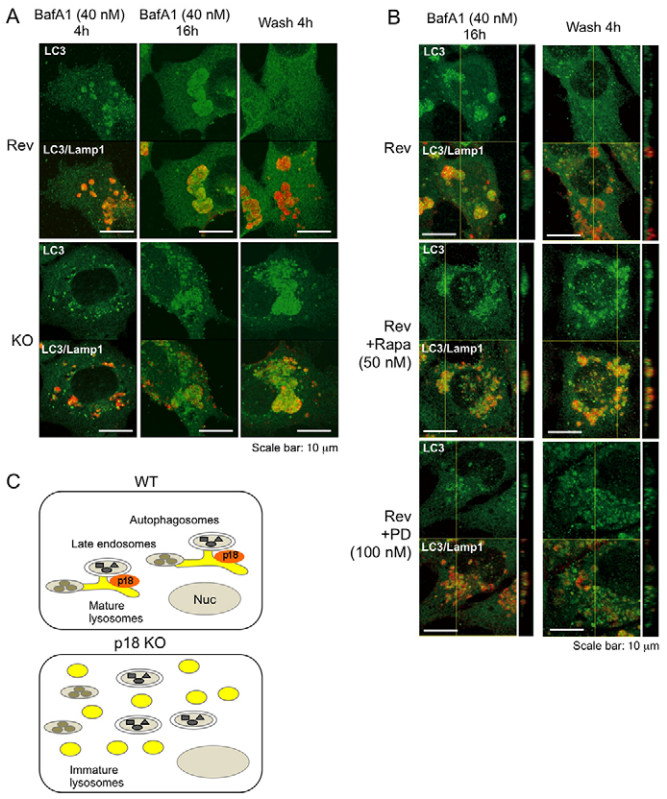

Fig. 8. Effects of inhibitors of mTORC1 and MAPK pathways on interaction between lysosomes and autophagosomes. (**A**) LC3-GFP was transiently expressed in p18 re-expressing cells (Rev) that stably express Lamp1-mCherry. Cells were incubated with BafA1 in the absence or presence of rapamycin (Rapa) or PD0325901 (PD) for 16 h, and BafA1 was washed out for an additional 4 h by replacing the media. At the indicated time points, localizations of LC3 and Lamp1 signals were analyzed using confocal microscopy. Z-stack images and Z-axis images at the yellow lines are shown. (**B**) LC3-GFP was transiently expressed in p18 KO cells (KO) and p18 re-expressing cells (Rev) that stably express Lamp1-mCherry. Cells were incubated with Bafilomycin A1 (BafA1) for 4 h and 16 h, and BafA1 was washed out for an additional 4 h. At the indicated time points, localizations of LC3 and Lamp1 signals were analyzed using confocal microscopy. Z-stack images are shown. (**C**) A schematic model for the function of the p18 complex on lysosomes. Lysosomes conveying the p18 complex can functionally interact with their target organelles, such as autophagosomes and late endosomes.

Schekman, 2008). Therefore, it is possible that the functions of some components are directly or indirectly (e.g. through regulation of gene expression) modulated by activation of mTORC1 and/or MAPK pathway through the p18 complex on lysosomes. Identification of the specific targets of these pathways on lysosomes will be needed to clarify the molecular mechanisms underlying these events (Hsu et al., 2011). It has been demonstrated in yeast that the EGO complex, a yeast ortholog of the p18 complex, positively regulates the direct engulfment of cytoplasmic material into the lysosome, namely microautophagy, in accordance with TOR (Dubouloz et al., 2005). It is thus also possible that a similar mechanism is in place in mammalian system, although the precise molecular mechanisms remain unknown.

In p18 KO cells, we observed that immature lysosomes are diffusely distributed throughout the cytoplasm, suggesting that the transport of vesicles along microtubules may also be abrogated by loss of p18. Lysosomal positioning is crucial for the coordination of mTORC1 functions (Korolchuk et al., 2011). However, we observed no significant difference in the organization of microtubules or actin fibers, or in vesicle movement, between wild-type and mutant cells (data not shown). Therefore, we suggest that the aberrant distribution of immature lysosomes resulting from loss of p18 is more likely due to defects in lysosome maturation. It is possible that some components of the p18 complex serve as a 'tag' representing the cargo organelle, and such tag-bearing mature lysosomes are specifically transported to the perinuclear compartment along microtubules via dynein motors. Indeed, time-lapse analysis showed that the Lamp1/p18-positive tubular lysosomes moved rapidly along microtubules toward perinuclear compartments when they interacted with their target vesicles such as LC3-positive autophagosomes (supplementary material Movies 2–5).

In this study, we observed accumulation of autophagosomes upon loss of p18 in the epidermis, as well as in cultured cells. It is well established that autophagy is regulated by mTORC1 activity (Yang and Klionsky, 2010; Zoncu et al., 2011a). Under normal conditions, active mTORC1 phosphorylates and inactivates ATG proteins to suppress induction of autophagy (Hosokawa et al., 2009). However, we observed that the inhibition of lysosomal function with BafA1 treatment could induce accumulation of autophagosomes even in wild-type cells. This finding suggests that under normal conditions, autophagy is active, but autophagosomes are rapidly degraded by efficient fusion with lysosomes. Because our data indicate that the p18 pathway is involved in the activation of lysosome functions, it is likely that mTORC1 can regulate autophagy not only by suppressing initiation of autophagy but also by facilitating degradation of autophagosomes. If this is indeed the case, the inhibition of mTORC1 by starvation not only induces autophagy, but also inactivates lysosome function. If these events were to continue during starvation, cells would be unable to degrade autophagosomes to regenerate metabolic precursors. This would appear to conflict with the overall purpose of autophagy. However, a recent study demonstrated that mTORC1 signaling is reactivated by prolonged starvation, and this increased mTORC1 activity attenuates autophagy and induces reformation of lysosomes (Yu et al., 2010). In this study, we also observed reactivation of mTORC1 during longer starvation periods, which occurred concomitantly with degradation of autophagosomes (supplementary material Fig. S2). By contrast, there was no reactivation of mTORC1 in p18 KO cells, which have very low levels of mTORC1 activity, resulting in a significant delay in autophagosome degradation. These findings shed new light on the regulatory mechanism of autophagy.

In the mutant epidermis, we observed reduced production of cholesterol, ceramides and SMPD1, all of which are secreted into the stratum corneum via lamellar bodies from the granular cells. The lamellar bodies are categorized as lysosome-related organelles (LRO) that share some features of late endosome/lysosomes (Raposo et al., 2007; Ridsdale et al., 2011), and cholesterol and ceramides are stored and processed by late endosomes (Bouwstra et al., 2003; Ganley and Pfeffer, 2006; Sobo et al., 2007). Thus, the dysfunction of lamellar bodies in the mutant epidermis suggests that the p18 complex is also involved in the regulation of LRO biogenesis. We also observed the accumulation of glycogen granules in mutant epidermal cells,

suggesting that breakdown of glycogen is largely mediated by lysosomes that contain acid glucosidase. Like these, the epidermal phenotypes caused by loss of p18 appeared to be largely associated with lysosomal dysfunction. Therefore, it is likely that, as a consequence of the accumulation of undigested or unprocessed materials (autophagosomes, nuclei, glycogen granules, etc.) as well as the attenuated secretion of extracellular components (cholesterol, ceramides, hydrolases), granular cells fail to undergo terminal differentiation into the stratum cornea.

In summary, we have shown here that the p18 complex on lysosomes plays a crucial role in controlling lysosome-mediated catabolic processes, which are required for maintenance of cell homeostasis and development of particular cell types. Because the endosome system is crucial for infection by various pathogens, and has been implicated in various human hereditary diseases such as lysosome storage diseases (Settembre et al., 2008), further analysis of p18-mediated function may provide new opportunities for therapeutic intervention in various human diseases.

Materials and Methods

Generation of K5-*p18*$^{fl/fl}$ mice

The *loxP* sites were introduced into the 5′ and 3′ sides of exon 1 of the *p18* gene by homologous recombination in ES cells (Fig. 1). ES cells of floxed clones identified by PCR were used to generate mice carrying floxed (*p18*^{fl}) *p18* alleles. *K5-Cre* transgenic mice (Tarutani et al., 1997) were mated with *p18*$^{flox/flox}$ mice. F2 offspring carrying the *p18*$^{flox/flox}$ locus and the *K5-Cre* transgene (*K5-Cre-p18*$^{flox/flox}$), and their littermates carrying no *K5-Cre* transgene (*p18*$^{flox/flox}$), were used as *K5 p18*-KO mice and control mice, respectively. Genotypes were confirmed by detection of *K5-Cre* and the *p18*^{flox} locus by allele-specific PCR analysis of genomic DNA from tail snips (Yagi et al., 2007). Primer sequences used are as follows: p18-forward (1803f), 5′-AAG GAT TCG GAG TTA GAG ACT AGG AC-3′; p18-reverse (2409r), 5′-TGA GGA TTC GAG TGG TGA GAT ACG A-3′; K5-Cre-forward (286f), 5′-AAC ATG CTT CAT CGT CGG TCC GG-3′; K5-Cre-reverse (922r), 5′-CGG TAT TGA AAC TCC AGC GCG G-3′. Mice were handled and maintained according to the Osaka University guidelines for animal experimentation.

Reagents and antibodies

Rapamycin was purchased from Santa Cruz Biotechnology, Inc. Filipin was obtained from Polyscience, Inc. Bafilomycin A1 was obtained form Sigma-Aldrich. Alexa Fluor 488-conjugated BSA (488 BSA) and self-quenched red BODIPY dye-conjugated BSA (DQ Red BSA) were purchased from Molecular Probes. An anti-p18 antibody was generated as described previously (Nada et al., 2009). Anti-laminin α3 antibody was kindly provided by K. Sekiguchi (Osaka University). Other antibodies used were obtained commercially: anti-keratin 1, anti-keratin 5 and anti-Filaggrin (Covance); anti-Ki67 (Novocastra); anti-claudin-1 (Zymed); anti-E-cadherin (BD Transduction Laboratories), anti-LAMP1(1D4B), anti-SMPD1, anti-cathepsin D1 and anti-GAPDH(6C5) (Santa Cruz Biotechnology, Inc.); anti-LC3 and anti-p62 (MBL, Japan); anti-β-tubulin (Sigma-Aldrich); anti-LAMTOR1 (p18), anti-S6K and anti-phosphoS6K (Cell Signaling). Horseradish peroxidase (HRP)-conjugated anti-rabbit, mouse IgG and anti-rat antibodies were obtained from Invitrogen, Bethyl Laboratories and Zymed, respectively. Alexa Fluor 566- and Alexa Fluor 694-conjugated anti-rabbit IgGs and FITC-conjugated anti-mouse IgG were obtained from Molecular Probes.

Histological analysis

Tissues were excised from mice deeply anesthetized with 10% Nembutal. The samples were fixed in 4% paraformaldehyde in phosphate-buffered saline (PBS) overnight at 4℃ and were embedded in Tissue-Tek OCT compound (Sakura Finetek, Japan) after cryoprotection with 15% and 30% sucrose solutions. Fixed samples were then cut into 10-μm sections with a cryostat (CM3050; Leica) and were analyzed by hematoxylin-eosin (HE) staining and immunohistochemistry. Specimens were incubated with blocking solution (10% BSA in PBS) and then incubated with primary antibodies in blocking solution (50% Can Get Signal; TOYOBO, Japan), followed by incubation with labeled secondary antibodies. Nuclei were stained with TO-PRO®-3 iodide (Life Technologies). Immunofluorescence histochemistry was performed as described previously (Koike et al., 2003; Yagi et al., 2007). Labeled sections were mounted under coverslips and examined by confocal laser-scanning microscopy (Olympus, FV-1000). TUNEL was performed using DeadEnd Fluorometric TUNEL system (Promega). Thin layer chromatography analysis of lipids in the epidermis was carried out by Toray Research Center (Tokyo, Japan). For epidermal barrier assay, embryos (E18.5) were incubated for 9 h at 37℃ in staining solution (1.3 mM $MgCl_2$, 100 mM $NaPO_4$, 3 mM $K_3Fe(CN)_6$, 3 mM $K_4Fe(CN)_6$ and 1 mg/ml X-Gal, pH 4.5) and stained embryos were photographed (Hardman et al., 1998).

Electron microscopy

Transmission electron microscopy was performed as described previously (Koike et al., 2003). Briefly, embryos were immersed in 2% glutaraldehyde/2% paraformaldehyde buffered with 0.1 M phosphate buffer (pH 7.2) and fixed overnight (or longer) at 4℃. Embryos were post-fixed with 1% OsO_4 in 0.1 M phosphate buffer, block-stained with a 2% aqueous solution of uranyl acetate, dehydrated with a graded series of ethanol and embedded in Epon 812. Ultrathin sections were cut with an ultramicrotome (Ultracut N; Reichert-Nissei), stained with uranyl acetate and lead citrate, and observed with a JEM-1011 electron microscope (JEOL).

Cell culture

Skin from newborn mice was treated with 0.05% collagenase A in Epilife Medium (GIBCO) for 24 h at 4℃, and the epidermis was peeled away from the dermis and trypsinized for 10 min at 37℃. Keratinocytes were cultured on collagen type I-coated plates in keratinocyte growth medium (KGM, GIBCO) under low-oxygen conditions (3% O_2). Mouse embryonic fibroblasts (MEFs) were established from *p18*$^{flox/flox}$ embryos by immortalizing with SV40 large T antigen. *p18*$^{-/-}$ cells (KO) were generated by the expression of the Cre gene, and MEFs re-expressing p18 (Rev) were prepared by introducing *p18* cDNA. MEFs, KO cells and Rev cells were cultured in DMEM supplemented with 10% fetal bovine serum. Cells were grown at 37℃ in a humidified atmosphere containing 5% CO_2.

Western blot analysis

Whole cell lysates were prepared in ODG buffer [50 mM Tris-HCl, pH 7.4, 1 mM EDTA, 0.15 M NaCl, 5% (w/v) glycerol, 1% (w/v) NP-40, 20 mM NaF, 2% n-octyl-β-D-glucoside (ODG), 5 μM β-mercaptoethanol, 1 mM sodium orthovanadate, 0.1% leupeptin, 0.1% aprotinin and 1 mM PMSF]. Equal amounts of total protein were separated by SDS-PAGE and transferred onto nitrocellulose membranes. Membranes were blocked and incubated with primary antibodies, followed by incubation with HRP-conjugated secondary antibodies. Signals from immunopositive bands were visualized on X-ray film using an enhanced chemiluminescence system (Amersham).

Fluorescence analysis

Keratinocytes cultured in 24-well plates were fixed with 4% paraformaldehyde for 15 min at room temperature. After washing with Tris-buffered saline containing 0.1% Tween 20 (TTBS), the samples were incubated with 5% BSA/TTBS, followed by incubation with primary antibodies in TTBS overnight at 4℃. After incubation with secondary antibodies for 45 min at room temperature, coverslips were mounted on glass slides. Cell lines were seeded onto fibronectin-coated coverslips and were fixed in 4% formaldehyde, followed by blocking with 1% BSA in PBS. Endogenous proteins were detected by immunofluorescence staining. Fluorescence was observed using an Olympus IX81 confocal microscope controlled by FluoView FV1000 software. Signal intensities and areas were determined using MetaMorph software (Universal Imaging). To monitor behavior of LC3-positive autophagosomes and Lamp1-positive lysosomes, LC3-GFP and Lamp1-mCherry fusion proteins were expressed in cell lines. pEGFP-LC3 vector was kindly provided by T. Yoshimori (Osaka University) and pmCherry-Lamp1 vector was generated by inserting Lamp1 cDNA into pmCherry vector (Clontech). For live-cell imaging, cells were seeded onto a 35 mm-diameter glass-bottom dishes coated with collagen or fibronectin in DMEM (phenol red-free) and monitored using an Olympus IX71 microscope equipped with a CoolSNAP HQ camera (Roper Scientific, Trenton, NJ) controlled by Metamorph software (Universal Imaging, West Chester, PA).

Acknowledgements

We thank Dr K. Sekiguchi for the generous gift of anti-laminin α3 antibody, T. Yoshimori for the generous gift of pEGFP-LC3 vector and for technical assistance and Ms H. Ohmori for electron-microscopic analysis.

Author contributions

T.S.-N. designed the experiments and analyzed mutant epidermis and keratinocyte cultures; S.N. generated mutant mice and performed in vitro experiments in cell lines; M.K. genotyped the mice and performed histology; Y.T. analyzed lysosomal function; S.M. analyzed expression of lysosomal proteins. C.O. assisted gene transfer experiments; M.O. designed the experiments and wrote the paper.

Funding

This study was supported in part by the Uehara Foundation and a Grant-in-Aid for scientific research from the Ministry of Education, Culture, Sports, Science and Technology of Japan.

Supplementary material available online at
http://jcs.biologists.org/lookup/suppl/doi:10.1242/jcs.121913/-/DC1

References

Bar-Peled, L., Schweitzer, L. D., Zoncu, R. and Sabatini, D. M. (2012). Ragulator is a GEF for the rag GTPases that signal amino acid levels to mTORC1. *Cell* **150**, 1196-1208.

Bohn, G., Allroth, A., Brandes, G., Thiel, J., Glocker, E., Schäffer, A. A., Rathinam, C., Taub, N., Teis, D., Zeidler, C. et al. (2007). A novel human primary immunodeficiency syndrome caused by deficiency of the endosomal adaptor protein p14. *Nat. Med.* **13**, 38-45.

Bonifacino, J. S. (2004). Insights into the biogenesis of lysosome-related organelles from the study of the Hermansky-Pudlak syndrome. *Ann. N. Y. Acad. Sci.* **1038**, 103-114.

Bonifacino, J. S. and Rojas, R. (2006). Retrograde transport from endosomes to the trans-Golgi network. *Nat. Rev. Mol. Cell Biol.* **7**, 568-579.

Bouwstra, J. A., Honeywell-Nguyen, P. L., Gooris, G. S. and Ponec, M. (2003). Structure of the skin barrier and its modulation by vesicular formulations. *Prog. Lipid Res.* **42**, 1-36.

Dell'Angelica, E. C., Mullins, C., Caplan, S. and Bonifacino, J. S. (2000). Lysosome-related organelles. *FASEB J.* **14**, 1265-1278.

Dubouloz, F., Deloche, O., Wanke, V., Cameroni, E. and De Virgilio, C. (2005). The TOR and EGO protein complexes orchestrate microautophagy in yeast. *Mol. Cell* **19**, 15-26.

Falguières, T., Luyet, P. P., Bissig, C., Scott, C. C., Velluz, M. C. and Gruenberg, J. (2008). In vitro budding of intralumenal vesicles into late endosomes is regulated by Alix and Tsg101. *Mol. Biol. Cell* **19**, 4942-4955.

Falguières, T., Luyet, P. P. and Gruenberg, J. (2009). Molecular assemblies and membrane domains in multivesicular endosome dynamics. *Exp. Cell Res.* **315**, 1567-1573.

Ganley, I. G. and Pfeffer, S. R. (2006). Cholesterol accumulation sequesters Rab9 and disrupts late endosome function in NPC1-deficient cells. *J. Biol. Chem.* **281**, 17890-17899.

Guillaumot, P., Luquain, C., Malek, M., Huber, A. L., Brugière, S., Garin, J., Grunwald, D., Régnier, D., Pétrilli, V., Lefai, E. et al. (2010). Pdro, a protein associated with late endosomes and lysosomes and implicated in cellular cholesterol homeostasis. *PLoS ONE* **5**, e10977.

Harada, A., Takei, Y., Kanai, Y., Tanaka, Y., Nonaka, S. and Hirokawa, N. (1998). Golgi vesiculation and lysosome dispersion in cells lacking cytoplasmic dynein. *J. Cell Biol.* **141**, 51-59.

Hardman, M. J., Sisi, P., Banbury, D. N. and Byrne, C. (1998). Patterned acquisition of skin barrier function during development. *Development* **125**, 1541-1552.

Hosokawa, N., Hara, T., Kaizuka, T., Kishi, C., Takamura, A., Miura, Y., Iemura, S., Natsume, T., Takehana, K., Yamada, N. et al. (2009). Nutrient-dependent mTORC1 association with the ULK1-Atg13-FIP200 complex required for autophagy. *Mol. Biol. Cell* **20**, 1981-1991.

Hsu, P. P., Kang, S. A., Rameseder, J., Zhang, Y., Ottina, K. A., Lim, D., Peterson, T. R., Choi, Y., Gray, N. S., Yaffe, M. B. et al. (2011). The mTOR-regulated phosphoproteome reveals a mechanism of mTORC1-mediated inhibition of growth factor signaling. *Science* **332**, 1317-1322.

Huotari, J. and Helenius, A. (2011). Endosome maturation. *EMBO J.* **30**, 3481-3500.

Jahreiss, L., Menzies, F. M. and Rubinsztein, D. C. (2008). The itinerary of autophagosomes: from peripheral formation to kiss-and-run fusion with lysosomes. *Traffic* **9**, 574-587.

Johannes, L. and Wunder, C. (2011). The SNXy flavours of endosomal sorting. *Nat. Cell Biol.* **13**, 884-886.

Kogan, K., Spear, E. D., Kaiser, C. A. and Fass, D. (2010). Structural conservation of components in the amino acid sensing branch of the TOR pathway in yeast and mammals. *J. Mol. Biol.* **402**, 388-398.

Koike, M., Shibata, M., Ohsawa, Y., Nakanishi, H., Koga, T., Kametaka, S., Waguri, S., Momoi, T., Kominami, E., Peters, C. et al. (2003). Involvement of two different cell death pathways in retinal atrophy of cathepsin D-deficient mice. *Mol. Cell. Neurosci.* **22**, 146-161.

Korolchuk, V. I., Saiki, S., Lichtenberg, M., Siddiqi, F. H., Roberts, E. A., Imarisio, S., Jahreiss, L., Sarkar, S., Futter, M., Menzies, F. M. et al. (2011). Lysosomal positioning coordinates cellular nutrient responses. *Nat. Cell Biol.* **13**, 453-460.

Luzio, J. P., Pryor, P. R. and Bright, N. A. (2007). Lysosomes: fusion and function. *Nat. Rev. Mol. Cell Biol.* **8**, 622-632.

Malek, M., Guillaumot, P., Huber, A. L., Lebeau, J., Pétrilli, V., Kfoury, A., Mikaelian, I., Renno, T. and Manié, S. N. (2012). LAMTOR1 depletion induces p53-dependent apoptosis via aberrant lysosomal activation. *Cell Death Dis.* **3**, e300.

Miaczynska, M., Pelkmans, L. and Zerial, M. (2004). Not just a sink: endosomes in control of signal transduction. *Curr. Opin. Cell Biol.* **16**, 400-406.

Mizushima, N., Yoshimori, T. and Ohsumi, Y. (2011). The role of Atg proteins in autophagosome formation. *Annu. Rev. Cell Dev. Biol.* **27**, 107-132.

Nada, S., Hondo, A., Kasai, A., Koike, M., Saito, K., Uchiyama, Y. and Okada, M. (2009). The novel lipid raft adaptor p18 controls endosome dynamics by anchoring the MEK-ERK pathway to late endosomes. *EMBO J.* **28**, 477-489.

Raposo, G., Marks, M. S. and Cutler, D. F. (2007). Lysosome-related organelles: driving post-Golgi compartments into specialisation. *Curr. Opin. Cell Biol.* **19**, 394-401.

Ridsdale, R., Na, C. L., Xu, Y., Greis, K. D. and Weaver, T. (2011). Comparative proteomic analysis of lung lamellar bodies and lysosome-related organelles. *PLoS ONE* **6**, e16482.

Sancak, Y., Bar-Peled, L., Zoncu, R., Markhard, A. L., Nada, S. and Sabatini, D. M. (2010). Ragulator-Rag complex targets mTORC1 to the lysosomal surface and is necessary for its activation by amino acids. *Cell* **141**, 290-303.

Settembre, C., Fraldi, A., Rubinsztein, D. C. and Ballabio, A. (2008). Lysosomal storage diseases as disorders of autophagy. *Autophagy* **4**, 113-114.

Sobo, K., Le Blanc, I., Luyet, P. P., Fivaz, M., Ferguson, C., Parton, R. G., Gruenberg, J. and van der Goot, F. G. (2007). Late endosomal cholesterol accumulation leads to impaired intra-endosomal trafficking. *PLoS ONE* **2**, e851.

Takahashi, Y., Nada, S., Mori, S., Soma-Nagae, T., Oneyama, C. and Okada, M. (2012). The late endosome/lysosome-anchored p18-mTORC1 pathway controls terminal maturation of lysosomes. *Biochem. Biophys. Res. Commun.* **417**, 1151-1157.

Tarutani, M., Itami, S., Okabe, M., Ikawa, M., Tezuka, T., Yoshikawa, K., Kinoshita, T. and Takeda, J. (1997). Tissue-specific knockout of the mouse Pig-a gene reveals important roles for GPI-anchored proteins in skin development. *Proc. Natl. Acad. Sci. USA* **94**, 7400-7405.

Teis, D., Wunderlich, W. and Huber, L. A. (2002). Localization of the MP1-MAPK scaffold complex to endosomes is mediated by p14 and required for signal transduction. *Dev. Cell* **3**, 803-814.

Teis, D., Taub, N., Kurzbauer, R., Hilber, D., de Araujo, M. E., Erlacher, M., Offterdinger, M., Villunger, A., Geley, S., Bohn, G. et al. (2006). p14-MP1-MEK1 signaling regulates endosomal traffic and cellular proliferation during tissue homeostasis. *J. Cell Biol.* **175**, 861-868.

Wickner, W. and Schekman, R. (2008). Membrane fusion. *Nat. Struct. Mol. Biol.* **15**, 658-664.

Yagi, R., Waguri, S., Sumikawa, Y., Nada, S., Oneyama, C., Itami, S., Schmedt, C., Uchiyama, Y. and Okada, M. (2007). C-terminal Src kinase controls development and maintenance of mouse squamous epithelia. *EMBO J.* **26**, 1234-1244.

Yamamoto, A., Tagawa, Y., Yoshimori, T., Moriyama, Y., Masaki, R. and Tashiro, Y. (1998). Bafilomycin A1 prevents maturation of autophagic vacuoles by inhibiting fusion between autophagosomes and lysosomes in rat hepatoma cell line, H-4-II-E cells. *Cell Struct. Funct.* **23**, 33-42.

Yang, Z. and Klionsky, D. J. (2010). Eaten alive: a history of macroautophagy. *Nat. Cell Biol.* **12**, 814-822.

Yu, L., McPhee, C. K., Zheng, L., Mardones, G. A., Rong, Y., Peng, J., Mi, N., Zhao, Y., Liu, Z., Wan, F. et al. (2010). Termination of autophagy and reformation of lysosomes regulated by mTOR. *Nature* **465**, 942-946.

Zoncu, R., Efeyan, A. and Sabatini, D. M. (2011a). mTOR: from growth signal integration to cancer, diabetes and ageing. *Nat. Rev. Mol. Cell Biol.* **12**, 21-35.

Zoncu, R., Bar-Peled, L., Efeyan, A., Wang, S., Sancak, Y. and Sabatini, D. M. (2011b). mTORC1 senses lysosomal amino acids through an inside-out mechanism that requires the vacuolar H(+)-ATPase. *Science* **334**, 678-683.